Active Vibration Control Using Piezostack Based Mount
압전작동기 마운트를 이용한 능동진동제어

Vien-Quoc Nguyen*, Sang-Min Choi*, Yong-Seok Paeng*, Young-Min Han**,
Seung-Bok Choi † and Seok-Jun Moon***
벤 큐 오 · 최 상 민 · 팽 용 석 · 한 영 민 · 최 승 복 · 문 석 준

Key Words : Hybrid Mount(하이브리드 마운트), Piezostack Actuator(압전작동기), Feed-forward Control(앞먹임 제어기)

ABSTRACT

This paper presents vibration control performance of an active hybrid mount featuring piezostack actuators. The proposed hybrid mount is devised by adopting piezostack as an active actuator and rubber as a passive element. After experimentally identifying actuating force characteristics of the piezostack and dynamic characteristics of the rubber, the hybrid mount was designed and manufactured. Subsequently, a vibration control system with a specific mass loading is constructed, and its governing equations of motion are derived. In order to actively attenuate vibration transmitted from the base, a feedforward controller is formulated and experimentally realized. Vibration control responses are then evaluated in time and frequency domains.

1. INTRODUCTION

In general, mounts are used to attenuate shocks and vibrations of dynamic systems for many applications such as naval equipments subjected to severe dynamic environments. Many types of passive mount have been used to achieve this purpose. A rubber mount is one of the passive mounts which is widely used due to its efficient vibration isolation performance against non-resonant and high frequency excitation. However, the passive rubber mount cannot exert good performance at some frequency regions, especially at resonant frequencies.

This performance limitation of the passive mount leads to the study on active and semi-active mounts featuring smart materials which include electro-rheological fluid [4-6], magneto-rheological fluid [7] piezoelectric materials [2,3] and shape memory alloys [8]. Among these, the piezoelectric material is the most promising candidate because of its fast response and easy controllability. However, the approach to directly bond the piezoelectric actuator on structures is not effective for large-sized structures under severe vibration loading such as equipments installed in naval vessels.

The main objective of this work is to propose a new type of active hybrid mount which can operate in wide frequency range, and its control performance is experimentally evaluated with a vibration system. The proposed active hybrid mount consists of one passive rubber element and two active piezostack actuators. A conventional rubber mount manufactured for naval vessels is adopted for the passive element, and its dynamic characteristics are evaluated. After identifying actuating force of the piezostack actuators, the hybrid mount is manufactured and applied to the vibration system with a lumped mass. The governing equations of motion of the proposed system is derived and followed by the synthesis of a simple feedforward control algorithm to attenuate vibration from the base. In wide frequency range from 20Hz to 1000Hz, vibration control performance is experimentally evaluated in time domain. In addition, transmitted forces are demonstrated in frequency domain.

2. MOUNT CONFIGURATION

Fig. 1 shows the configuration of the proposed hybrid mount which consists of piezostack actuators, rubber element and intermediate mass. As shown in the figure, two piezostack actuators located in parallel are combined with the rubber element in serial connection to prevent severe excitation. It is noted that the proposed hybrid

† 교신저자; 정회원, 인하대학교 기계공학부
E-mail: seungbok@inha.ac.kr
Tel: (032) 872-7925, Fax: (032) 868-1716

* 정회원, 인하대학교 대학원 기계공학과

** 정회원, 인하대학교 기계공학부

*** 정회원, 한국기계연구원 e-엔지니어링연구센터

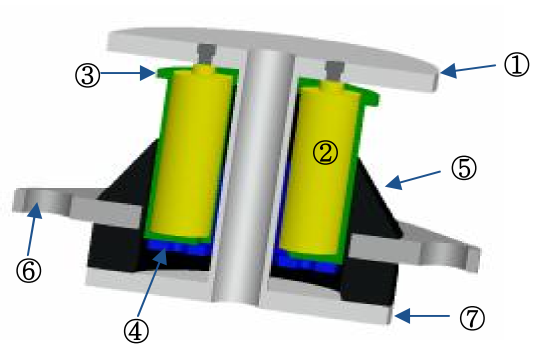

① Top Plate ② Piezostack Actuator
③ Intermediate Plate ④ Inertial Mass
⑤ Rubber Element ⑥ Insert Plate
⑦ Center Plate

Fig. 1 Configuration of the hybrid mount

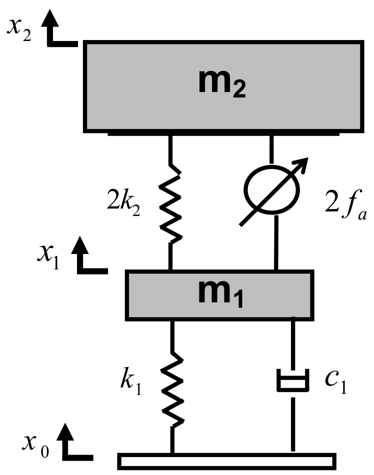

Fig. 2 Mechanical model of the hybrid mount

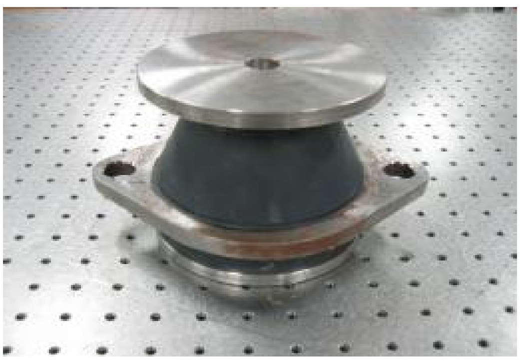

Fig. 3 A photograph of the manufactured hybrid mount

Table 1: Specification of MIL-STD-167-1A

Freq. (Hz)	20	50	100	200	500	1000
Acc. (m/s^2)	0.4737	1.1843	2.3687	4.7374	11.8435	23.6871

mount is very effective to severe dynamic environments with high shocks and vibrations, such as equipments installed in naval vessels.

In this work, a lumped mass is located on the top plate above the proposed mount. Excitations according to the military standard MIL-STD-167-1A shown in table 1 are transmitted through the insert plate from the base below the mount. The system of the proposed mount and the supported mass ('mount-mass system' for short) can be modeled as a two degree-of-freedom (2-DOF) system. From the mechanical model of the proposed system shown in Fig. 2, the governing equations of motion can be derived as follows:

$$\begin{aligned} m_1\ddot{x}_1 + c_1\dot{x}_1 + (k_1 + 2k_2)x_1 - k_2x_2 &= 2f_a + d \\ m_2\ddot{x}_2 + 2k_2x_2 - 2k_2x_1 &= -2f_a \end{aligned} \tag{1}$$

where x_1 and x_2 are the displacement of the inertial mass and of the supported mass, respectively; k_1 and c_1 are the stiffness and damping coefficient of the rubber element, respectively; k_2 in the stiffness of the piezostack actuators; d is the excitation from the base and determined by $c_1\dot{x}_0 + k_1x_0$; f_a is the force exerted by electric voltage to the piezostack actuators. These parameters can be experimentally determined. The Fig. 3 shows the photograph of the manufactured hybrid mount. In this work, the mass m_1 and m_2 are chosen to be 1.7kg and 50kg, respectively.

3. PARAMETER IDENTIFICATION

In this work, the rubber element is designed and manufactured under consideration of mounting environment of naval equipment. Its loading range is from 50 to 200kg. In general, the characteristics of the rubber are changed in accordance with upper load and vibration source. Therefore, the dynamic stiffness and damping coefficient can be experimentally determined by using Kelvin-Voigt model as follows:

$$k_d(j\omega) = k_r + j\omega c_r \tag{2}$$

where k_d is dynamic stiffness, k_r the static stiffness, c_r the damping constant, and ω the excitation frequency. Fig. 4 shows a schematic diagram of the test equipment for the rubber element. In this work, the measured stiffness and damping coefficient are 160447N/m and 537Ns/m, respectively.

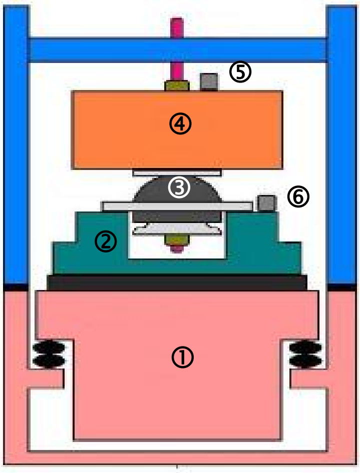

① Shaker ② Jig
③ Rubber mount ④ 50kg mass
⑤,⑥ Accelerometers

Fig. 4 Test equipment for the rubber element

As early mentioned, in order to improve vibration isolating performance of the rubber, the piezostack actuators are adopted in this work. Its electromechanical behavior, providing actuation along the polarized direction, can be expressed as follows:

$$D = \varepsilon_{33}E + d_{33}T \tag{3}$$

$$S = d_{33}E + \frac{1}{c}T \tag{4}$$

In the above, D is the electrical displacement, E the electric field, T the stress, S the strain, ε_{33} the dielectric constant at zero stress, d_{33} the piezoelectric charge constant, and c the elastic modulus at zero electric field. Then the constitutive equation of the piezostack actuator stack by n piezoelectric layers can be derived from the equation as follows:

$$\begin{aligned} f_p(t) &= AT = AcS - Acd_{33}E \\ &= Ac\frac{\delta(t)}{l} - Acd_{33}\frac{V(t)}{l} \\ &= k_p\delta(t) - \alpha V(t) = k_p\delta(t) - f_a(t) \end{aligned} \tag{5}$$

where f_p(t) is the load applied to the piezostack, A the cross-sectional area of the piezoelectric element, l the length of the piezostack, k_p (= Ac/l) the spring constant, α (= Acd_{33}/l) the proportional constant, and $f_a(t)$ (= $\alpha V(t)$) the force exerted by the electric voltage $V(t)$. The stroke $\delta(t)$ of the piezostack can be predicted from Eq. (6):

$$\delta(t) = \frac{1}{k_p}\left[\alpha V(t) + f_p(t)\right] \tag{6}$$

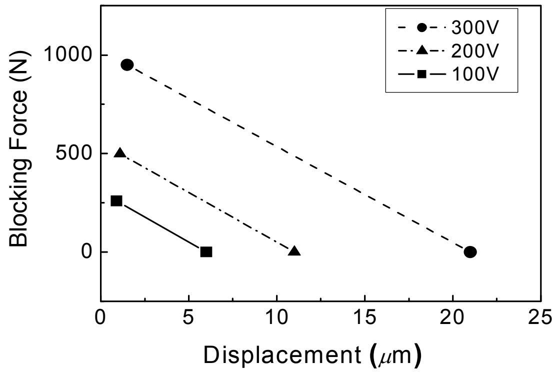

(a) Piezostack actuator 1

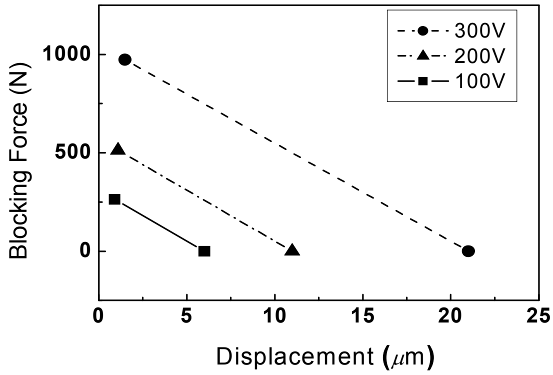

(b) Piezostack actuator 2

Fig. 5 Measured blocking force of the piezostacks

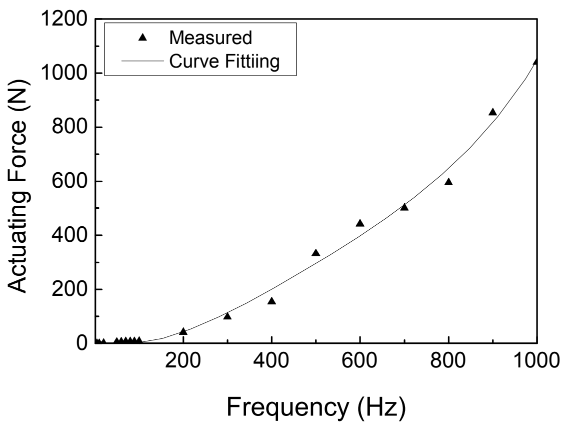

Fig. 6 Actuating force exerted by the piezostacks

Fig. 5 presents experimental results of blocking force produced by the piezostack actuators. The average value of the spring constant and proportional constant of the piezostack actuators is 47MN/m and 2.4N/V, respectively. The maximum blocking force is evaluated to be about 1000N at the input voltage of 300V. The results also show that the two piezostack actuators have nearly the same stiffness. Fig. 6 shows the measured actuating force with respect to the frequency. It is observed that the force increases proportionally to the square of the frequency.

4. CONTROLLER DESIGN

In this work, control purpose is to suppress vibration of the supported mass transmitted from the base. By defining a state vector $\mathbf{x}=\begin{bmatrix} x_1 & x_2 & \dot{x}_1 & \dot{x}_2 \end{bmatrix}^T$, the governing equations of motion (1) of the mount-mass system can be rewritten in state-space representation as follows

$$\begin{aligned} \dot{x}(t) &= \mathbf{A}x(t)+\mathbf{B}u(t)+\mathbf{\Gamma}d(t) \\ z(t) &= \mathbf{C}x(t) \\ y(t) &= \dot{z}(t) \end{aligned} \tag{7}$$

where $z(t)$ and $y(t)$ is the velocity and the acceleration of the supported mass m_2, , respectively; the input $u(t)$ is voltage applied to the piezostack actuators; $d(t)$ is disturbance which is the excitation from the base. The matrices **A**, **B**, **C**, and **Γ** are given by

$$\mathbf{A}=\begin{bmatrix} 0 & 0 & 1 & 0 \\ 0 & 0 & 0 & 1 \\ \dfrac{-(k_1+2k_2)}{m_1} & \dfrac{2k_2}{m_1} & \dfrac{-c_1}{m_1} & 0 \\ \dfrac{2k_2}{m_2} & \dfrac{-2k_2}{m_2} & 0 & 0 \end{bmatrix}$$

$$\mathbf{B}=\begin{bmatrix} 0 \\ 0 \\ \dfrac{2\alpha}{m_1} \\ \dfrac{-2\alpha}{m_2} \end{bmatrix}, \quad \mathbf{\Gamma}=\begin{bmatrix} 0 \\ 0 \\ \dfrac{-1}{m_1} \\ 0 \end{bmatrix} \tag{8}$$

$$\mathbf{C}=\begin{bmatrix} 0 & 0 & 0 & 1 \end{bmatrix}$$

The feedforward controller is formulated as follows:

$$u(t)=-\mathbf{K}d(t) \tag{9}$$

where **K** is the control gain. By substituting Eq. (9) into Eq. (7), we obtain

$$\dot{\mathbf{x}}(t)=\mathbf{A}\mathbf{x}(t)+(\mathbf{\Gamma}-\mathbf{B}\mathbf{K})d(t) \tag{10}$$

It would be ideal if we can make $(\mathbf{\Gamma}-\mathbf{B}\mathbf{K})=0$, in which there would be absolutely no influence of the disturbance $d(t)$ on the system. Unfortunately, in our system, since the number of inputs is less than that of the states, there is no selection of **K** which results in $(\mathbf{\Gamma}-\mathbf{B}\mathbf{K})=0$. However, **K** can be chosen to minimize the effect of the disturbance $d(t)$. In our case, since d and u are scalars, **K** must be scalar. Hence it can be tuned easily to obtain the best value in practice. The Fig. 7 shows the corresponding control block diagram of the proposed control system.

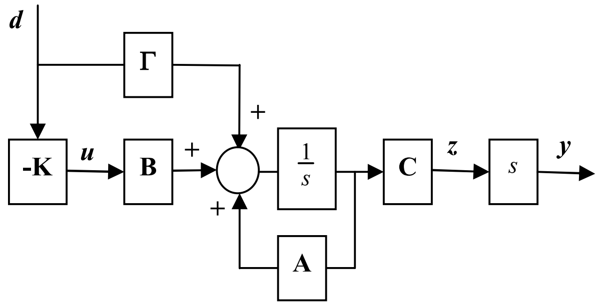

Fig. 7 Block diagram of the control system

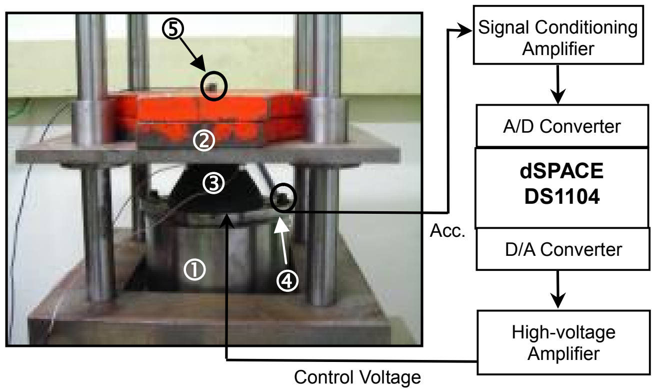

① Shaker + Jig ② 50kg mass
③ Hybrid mount ④,⑤ Accelerometers

Fig. 8 Experimental apparatus for vibration control

5. CONTROL RESULTS AND DISCUSSIONS

Fig. 8 shows experimental setup for vibration control. A 50kg mass is loaded on the upper plate above the mount, whose base plate is excited by an electromagnetic shaker. Two accelerometers are installed: one is on the shaker to measure the acceleration of the vibration source for feedforward control; the other is on the mass to monitor its vibration for evaluating the control performance.

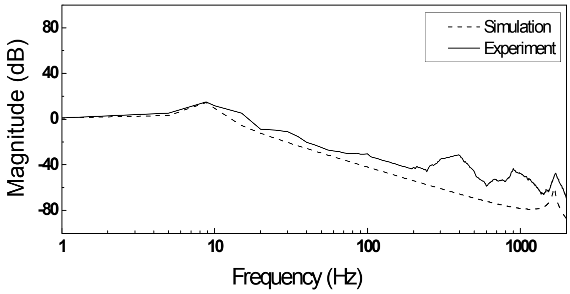

Fig. 9 Frequency response of the mount-mass system

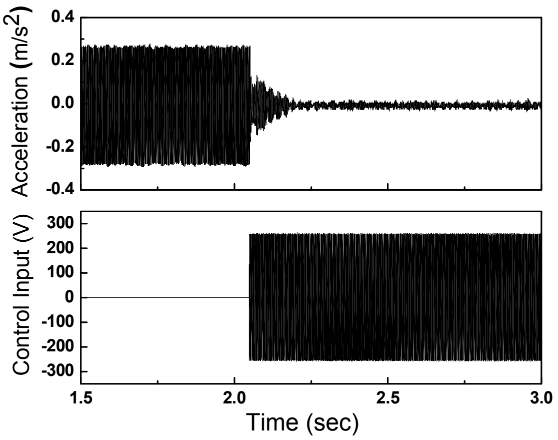

Fig. 10 Control response under excitation at 400 Hz

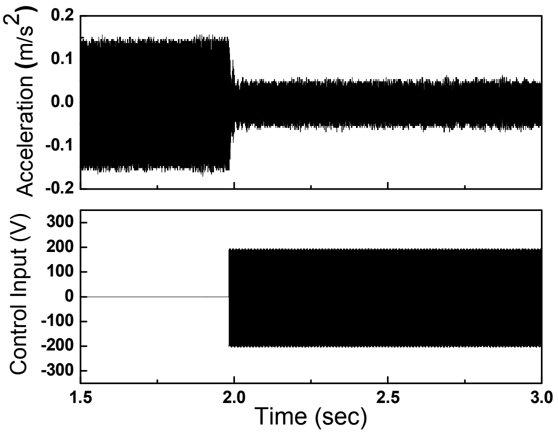

Fig. 11 Control response under excitation at 900 Hz

The controller is implemented by using dSPACE DSP board DS1104, in which some high-speed A/D and D/A converters are integrated. The sampling rate of the control system is chosen to be 10kHz. When the vibration is transmitted to the mount, the feedforward controller is activated to attenuate the vibration at the supported mass. The dynamic response signals are

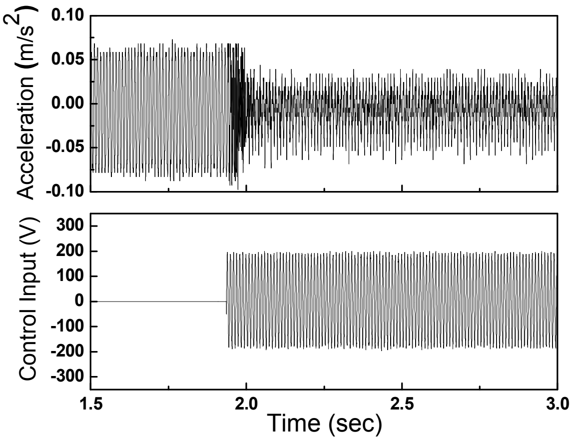

Fig. 12 Control response under excitation at 100 Hz

acquired from accelerometers at the supported mass and shaker via dSPACE DSP board DS1104. Fig. 9 shows the measured frequency response of the mount-mass system. From the simulation result, it is seen that two resonant frequencies are found at 8.78Hz and 1.2kHz which matches with the measured ones. It is noted that from 200Hz to 1000Hz, the real system has some resonant peaks in the frequency response due to the complicated structure of the load.

In the first vibration control experiment, the shaker is set to generate sinusoidal vibration at 400Hz with amplitude of 1.69μm. The corresponding excitation acceleration is 10.68m/s^2. Time response of the system is shown in Fig. 10. When the controller is not activated, the vibration at the mass is suppressed to 0.27m/s^2 or -31.86dB. The corresponding maximum displacement and transmitted force are 0.0432μm and 13.64N, respectively. After 2.05 seconds, the controller is activated. It can be seen that the acceleration is effectively reduced to 0.0152m/s^2 or -56.94dB in total (compared with the excitation). The corresponding displacement and transmitted force is reduced to 0.0024μm and 0.76N, respectively. The vibration of the mass in controlled case is 25.08dB lower than that in uncontrolled case. Fig. 11 presents the control performance under high frequency excitation at 900Hz. From the experimental results, it can be seen that acceleration of the supported mass is decreased 9.42dB by activating the proposed feedforward controller. In the low frequency at 100Hz, the vibration attenuation is favorable as shown in Fig. 12. Table 2 presents the decreased vibration levels in a wide

Table 2: Experimental results at several frequencies

Freq. (Hz)	Uncontrolled		Controlled	
	Acc (m/s^2)	dB	Acc (m/s^2)	dB
20	0.157	-8.75	0.147	-9.33
50	0.049	-9.89	0.041	-11.44
70	0.049	-30.70	0.047	-31.06
100	0.075	-30.54	0.028	-39.10
200	0.048	-40.21	0.029	-44.64
300	0.128	-35.15	0.018	-52.16
400	0.273	-31.86	0.015	-56.94
500	0.062	-45.94	0.013	-59.54
600	0.016	-58.72	0.004	-70.55
700	0.036	-53.89	0.024	-57.46
800	0.040	-54.56	0.015	-63.13
900	0.147	-43.34	0.050	-52.76
1000	0.092	-47.54	0.022	-59.84

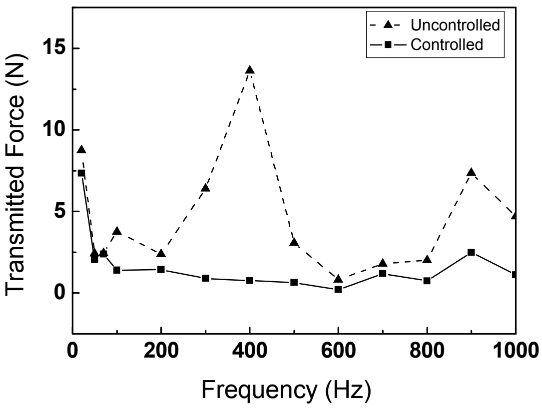

Fig. 13 Transmitted force in frequency domain

frequency range from 20 to 1000Hz, and the corresponding transmitted force is demonstrated in Fig. 13. From these results, it can be assured that the vibration control performance of the proposed hybrid mount is superior in wide frequency range. It is also noted that control performance below 100Hz is relatively low because of small inertial force of the piezostack actuator by low frequency excitation. The experimental results show that by using the proposed hybrid mount with a proper controller, the vibration isolating performance can be effectively achieved in wide frequency range.

6. CONCLUSION

In this paper, an active hybrid mount has been proposed for equipments subjected to severe dynamic environment such as naval vessels. By adopting piezostack actuators and rubber element, the proposed mount was designed and manufactured. A simple, but effective feedforward controller was formulated to suppress vibrations of a 50kg mass in a mount-mass system. Through experimental realization of the feedforward control, it has been demonstrated that the imposed vibrations were substantially reduced in wide frequency range from 20Hz to 1000Hz.

ACKNOWLEDGEMENT

This work was supported by Dual Technology Project directed by Korea Institute of Machinery & Materials (KIMM). This financial support is gratefully acknowledged.

REFERENCES

(1) Yunhe Y., Nagi G. N., Rao V. D., A literature review of automotive vehicle engine mounting systems. Mechanism and Machine Theory, 36, pp. 123-142, 2001

(2) Kim S. H., Choi S. B., Hong S. R., Han M. S., Vibration control of a flexible structure using a hybrid mount. International Jounal of Mechanical Sciences, 46, pp. 143-157, 2004

(3) Choi S. B., Hong S. R., Kim S. H., Beam vibration control via rubber and piezostack mounts: experimental work. Journal of Sound and Vibration, 273, pp. 1079-1086, 2004

(4) Hong S.R., Choi S.B., Jung W.J., Ham I.B., Kim D.K., Vibration control of an ER mount subjected to high static loads, Journal of Sound and Vibration. 242(4), pp. 740-748, 2001

(5) Choi S.H., Choi Y.T., Choi S.B., Cheong C.C., Performance analysis of an engine mount featuring ER fluids and piezoactuators, International Journal of Modern Physics B, 10(23), pp. 3143-3157, 1996

(6) Jung W.J., Jeong W.B., Hong S.R., Choi S.B., Vibration control of a flexible beam structure using squeeze-mode ER mount. Journal of Sound and Vibration, 273, pp. 185-199, 2004

(7) Hong S.R., Choi S.B., Vibration control of a structural system using magneto-rheological fluid mount. Journal of Intelligent Material Systems and Structures, 16, pp. 931-936, 2005

(8) Choi S.B., Cheong C.C., Vibration control of a flexible beam using SMA actuators. Journal of Guidance, Control, and Dynamics, 19(5), pp. 1178–1180, 1996

(9) Yook J.Y., Choi S.B., Sung K.G, Moon S.J., Design of hybrid mount using rubber element and piezoelectric actuator with application to vibration control. Transactions of the Korean Society for Noise and Vibration Engineering, Vol. 17, No. 5, pp. 390-397, 2007

(10) Paeng Y.S., Yook J.Y., Choi S.B., Moon S.J., Control performance of hybrid mount using electromagnetic actuator and PZT Actuator. Transactions of the Korean Society for Noise and Vibration Engineering, Vol. 17, No. 7, pp. 617-623, 2007